

DETC2007-35657

## POSITIVE FEEDBACK IN POWERED EXOSKELETONS: IMPROVED METABOLIC EFFICIENCY AT THE COST OF REDUCED STABILITY?

**James A. Norris**  
School of Biomedical  
Engineering & Sciences  
Winston-Salem, NC 27157

**Anthony P. Marsh\***  
Wake Forest University  
313 Reynolds Gymnasium  
Winston-Salem, NC 27109

**Kevin P. Granata**  
Virginia Tech

**Shane D. Ross**  
Virginia Tech  
224 Norris Hall  
Blacksburg, VA 24061

### ABSTRACT

A broad objective of many lower extremity exoskeletons is to allow the wearer to expend less of their own energy for locomotion. Existing exoskeleton control algorithms are based on positive feedback. Forces are generated to augment movement initiated by the wearer. Positive feedback, however, can have destabilizing effects in dynamic systems. In fact, stability in these lower extremity exoskeletons is achieved by relying on the wearer's neuromuscular system. Relying on the wearer to maintain stability may increase metabolic demand, which is counter productive to increasing efficiency. Thus, the goal of this study was to measure how a simple form of positive feedback that augments ankle push-off power affects both metabolic efficiency and dynamic walking stability. We developed a pair of powered ankle-foot orthoses (PAFOs) similar in design to Ferris, et al. (J. Appl. Biomech. 21, 189-197, 2005). Nine young healthy adults ( $23.3 \pm 1.6$  years) walked on a treadmill in the PAFOs under two conditions: (1) with and (2) without push-off power assistance. Metabolic energy expenditure was calculated using indirect calorimetry. Walking stability was quantified using techniques for studying stability of dynamic system trajectories. The maximum Lyapunov exponent for assessing local dynamic stability, and the maximum Floquet multiplier magnitude for assessing orbital stability were calculated from foot and shank kinematics for each condition. Greater Lyapunov exponents and Floquet multipliers indicate decreased stability. Walking with mechanically generated push-off power increased metabolic efficiency ( $2.58 \pm 0.39$  to  $2.97 \pm 0.38$ ,  $p < 0.01$ ), did not affect local dynamic stability ( $0.14 \pm 0.02$  to  $0.14 \pm 0.02$ ,  $p = 0.77$ ), but decreased orbital dynamic stability ( $0.43 \pm 0.03$  to  $0.48 \pm 0.06$ ,  $p = 0.05$ ). This study provides evidence that positive feedback can negatively affect stability. Further investigations into understanding stability of movement will be necessary for the design of controllers for powered lower extremity exoskeletons.

### 1 INTRODUCTION

Advances in robotic exoskeleton technology are catching up to the sci-fi dream of the wearable electro-mechanical suit that seamlessly augments the wearer's abilities. Incorporating additional energy from an alternate source than one's own neuromuscular system has wide appeal, whether to carry additional loads, replace functional losses associated with age or pathology, or aid rehabilitation and neurological retraining following injury. Early exoskeleton designs were limited by bulky actuators and energy sources with poor power to weight ratios. Significant progress has been made in actuator technology, new light-weight materials, and power sources with improved energy density. A critical component of powered exoskeletons is the intelligent control. Intelligent control senses the wearer's intentions and possibly their environment, and actuates the exoskeleton to achieve their desired goal. Intelligent control that unites the wearer and exoskeleton is still a rapidly evolving area.

Kazerooni et al. have developed a self-contained powered exoskeleton, the Berkley Lower Extremity Exoskeleton (BLEEX), that allows the wearer to carry a heavy load on their back while only feeling a small fraction of the actual load [1,2]. The control algorithm to actuate the exoskeleton relies solely on measurements from the exoskeleton, i.e., no sensors are required on the human or between the human and exoskeleton. The original concept driving the development of the BLEEX exoskeleton was to allow healthy soldiers to carry greater equipment loads while maintaining the maneuverability of legged locomotion. Kazerooni and colleagues have had success in terms of developing an algorithm that shadows the wearer's voluntary movements to provide exceptional maneuverability.

Another approach is to integrate physiologic data from the user into the control algorithm. HAL (Hybrid Assistive Limb), a self-contained powered exoskeleton, developed by Sankai et al. [3,4] has controllers to provide augmented force based on

\* Associate Professor and author of correspondence, Phone: (336) 758-4643, Fax: (336) 758-4680, Email: marshap@wfu.edu.

muscle surface electromyography (EMG). In addition to providing mechanical forces, the exoskeleton attempts to match the wearer's joint viscoelasticity. The wearer's joint viscoelasticity is estimated from on-line parameter identification methods.

Ferris et al. designed articulated lower extremity orthoses with pneumatic muscle actuators to provide additional power to the joints of the lower extremity during gait [5,6]. A goal of their work was to understand neurological adaptation to augmented power and aid rehabilitation of patients with neurological injuries. They showed that actuating pneumatic muscles in proportion to EMG causes a subject to change their recruitment pattern and kinematics. For example, when driving a plantarflexor actuator in proportion to plantarflexor muscle EMG, the plantarflexor muscle EMG decreased while plantarflexion range of motion increased. Unlike BLEEX and HAL, these powered orthoses were not designed to leave the laboratory or rehabilitation site and so are not self-contained.

In these examples of powered lower extremity exoskeletons and others in development (refer to [7] for a compilation of powered exoskeletons), force augmentation is achieved largely by positive feedback. Positive feedback, however, can have destabilizing effects in dynamic systems. Stability in these lower extremity exoskeletons is achieved by relying on the inherent stability of the human neuromuscular system. However, mechanically augmented forces based on positive feedback may affect stability. This is important because there are situations where augmenting force in a manner that reduces stability may be undesirable, e.g., in rehabilitation settings or for mobility assistance with older adults.

The goal of this study was to investigate how a simple control algorithm that augmented ankle power at push-off changed metabolic efficiency and walking stability. It was hypothesized that positive force augmentation at the ankle joint would increase the wearer's metabolic efficiency. A secondary hypothesis was that positive force augmentation would decrease the wearer's stability.

## 2 METHODS

### 2.1 Powered Ankle-Foot Orthoses

We built one pair of PAFOs based on designs by Ferris et al. [5]. The orthoses were made of 3/16<sup>th</sup>-inch polypropylene and fitted with aluminum attachment brackets (Figure 1). The PAFOs included removable 1/8<sup>th</sup>-inch foam liners to accommodate different subjects and Velcro straps to minimize relative motion between the subject's extremities and orthoses.

Electronic gyroscopes were rigidly attached to the foot and shank sections to measure sagittal-plane angular velocities. Inline load cells measured force produced by each plantarflexor pneumatic muscle. Signals were recorded at 100 Hz. The pneumatic muscles were actuated by delivering compressed air at 60psi through a small 5/3 solenoid valve. The mass of each orthosis as pictured in Figure 1 was 0.79 kg; for comparison, a standard sport shoe is around 0.4 kg.

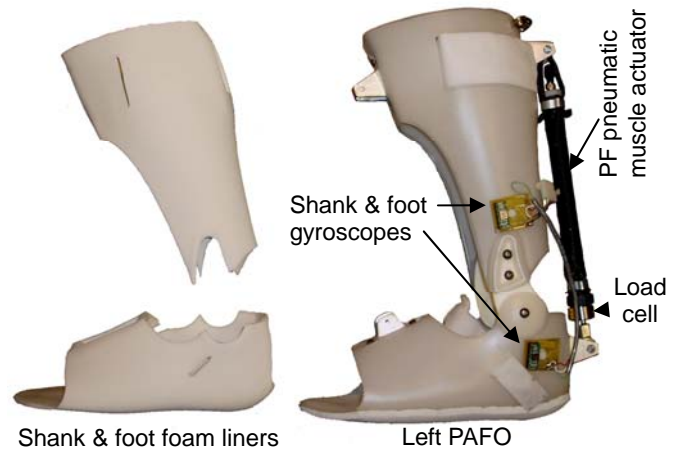
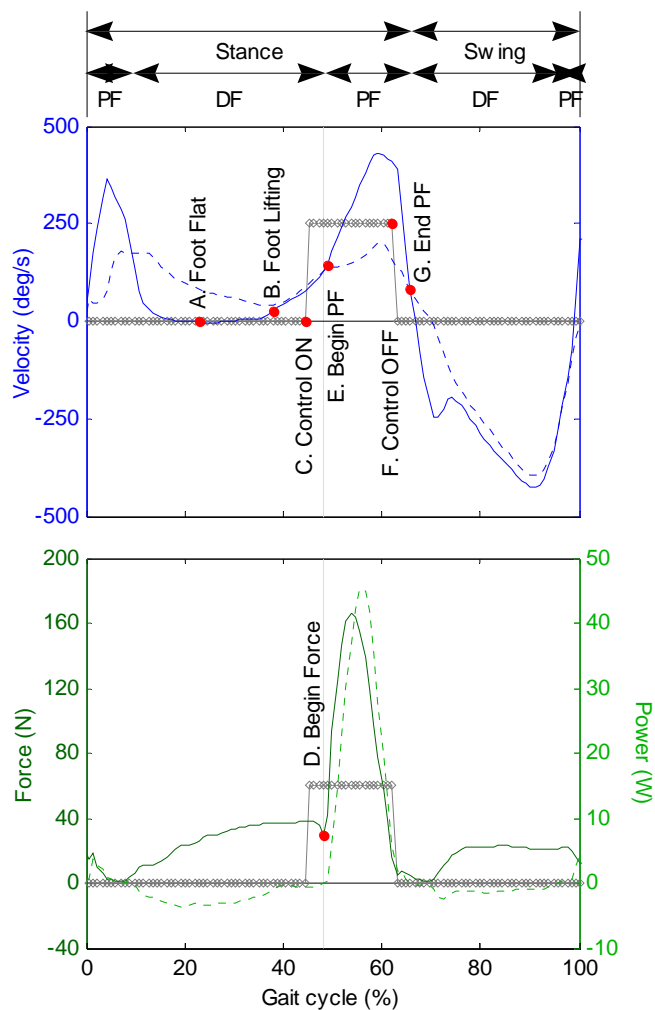


Figure 1. Foam liners and Powered AFO.

A simple control algorithm was developed to actuate the left and right pneumatic actuators to augment plantarflexion push-off power. Control of right and left sides were identical and independent of the contralateral limb. Therefore, the control algorithm will be presented for one side. First, foot-flat was defined when the magnitude of the foot angular velocity was below 20 deg/s for 100ms (Figure 2 – A). Next, the algorithm detected initiation of heel-lift (B). The control signal was turned on (C) after a subject-specific fixed-time delay following heel-lift. During acclimation trials, the time delay was adjusted in 10ms increments until the pneumatic muscle force associated with compressed air delivery (D) was aligned with the beginning of push-off (E). The pneumatic muscle generated forces creating a plantarflexion moment during push-off (E-G). This ensured the pneumatic muscles were doing positive mechanical work. Pneumatic muscle force is influenced by their length; therefore with the control valve fully open, force generation decreased due to shortening even though the supply pressure remained high. Lastly, the control signal was turned off (F) after 200ms, ensuring the pneumatic muscle was idle before toe-off.



**Figure 2.** Example of the foot (solid) and shank (dashed) angular velocities with control signal (solid-diamond), and force (solid) and power (dashed) provided by the pneumatic muscle during one stride. Vertical pink line in both plots marks the beginning of force production (D). Ankle is plantar-flexing (PF) when foot velocity is greater than shank velocity and dorsi-flexing (DF) when the opposite is true.

## 2.2 Quantifying Stability

Two approaches were applied to quantify stability of walking; local dynamic stability and orbital dynamic stability. Both techniques are based on analyzing stability of dynamic systems. A brief background on the theory of each approach is presented.

**Local dynamic stability.** As we walk we are constantly adjusting to small disturbances. Response to these disturbances may be used to quantify local dynamic stability [8-10]. At a given instant in time, the position and velocity of body segments are taken to represent the state of the system. How these states evolve in time defines a trajectory in state-space. An example of a three-dimensional trajectory is shown in Figure 3. A disturbance to a trajectory may evolve in three ways; it may (1) converge back to the undisturbed trajectory, indicating local stability, (2) diverge from the undisturbed trajectory, indicating local instability, or (3) parallel the undisturbed trajectory, i.e. neutral stability. A state-space is

multi-dimensional and as such there are indices of local stability, known as Lyapunov exponents [11]. There are as many Lyapunov exponents as there are dimensions in the state-space. However, with experimental data it is generally only possible to quantify stability of the least stable direction. This is acceptable since, hypothetically, a system is only as stable as its least stable direction. Quantifying the stability of the least stable direction is achieved by examining how the Euclidean distance between initially close states, or nearest neighbors, evolves in time [12]. For each pair of nearest neighbors in a data set, it is possible to calculate their separation with respect to time over finite-time intervals. In the case where the average separation exhibits an exponential relationship with time, the averaged behavior of nearby trajectories is quantified by the maximum Lyapunov exponent ( $\lambda_{\max}$ ) according to,

$$d(t) = d_o e^{\lambda_{\max} t} \quad (1)$$

where  $d(t)$  is the mean of the separation curves and  $d_o$  is the initial separation. Refer to discussions in [13,14] of how to proceed if the separation curves are not exponential with respect to time.

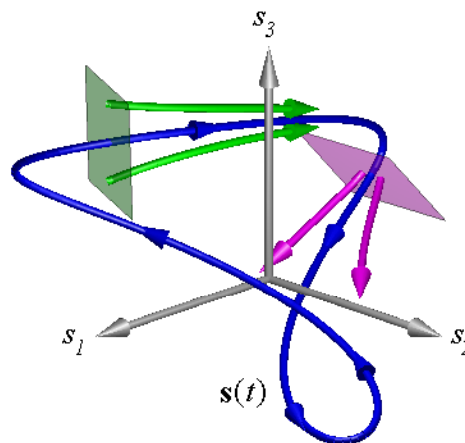


**Figure 3.** Locally stable (green) and unstable (magenta) regions along a hypothetical closed trajectory  $\mathbf{s}(t)$ . The shaded 2-d planes are orthogonal to the trajectory and the solid green and magenta disturbed trajectories are exponentially converging and diverging, respectively, from the undisturbed trajectory.

**Orbital dynamic stability.** Orbital stability of walking may be quantified by Floquet multipliers. Similar to local dynamic stability, the goal is to examine the sensitivity of state-space trajectories to small disturbances. While local stability can be analyzed for all trajectories of a system, orbital stability is a technique restricted to closed trajectories (i.e., periodic orbits) in the state-space. Quantifying orbital stability is based on evolution of the state at a discrete instant across subsequent cycles, thus reducing the question of stability of the periodic orbit to stability of an equilibrium point of a return map (Figure 4). Sampling the state at a discrete event of the gait cycle, such as heel-strike, defines a Poincaré section [15,16]. From dynamic systems theory, there is a function known as a Poincaré map,  $\mathbf{P}$ , that describes the evolution from the state at

the  $i^{\text{th}}$  intersection of the Poincaré section,  $\mathbf{s}_i$ , to the state at the subsequent intersection,  $\mathbf{s}_{i+1}$ ,

$$\mathbf{s}_{i+1} = \mathbf{P}(\mathbf{s}_i) \quad (2)$$

The equilibrium state defines a periodic motion that returns to itself upon subsequent intersections, i.e.  $\mathbf{s}_{eq} = \mathbf{P}(\mathbf{s}_{eq})$ . Linearizing the map about the equilibrium state yields a Jacobian matrix,  $\mathbf{J}_P$ , that describes the evolution of small disturbances about the equilibrium according to,

$$(\mathbf{s}_{i+1} - \mathbf{s}_{eq}) = \mathbf{J}_P (\mathbf{s}_i - \mathbf{s}_{eq}) \quad (3)$$

The eigenvalues of this Jacobian are known as Floquet multipliers,  $\phi$ , and they determine the stability of the periodic motion. There are as many Floquet multipliers as there are state-space dimensions minus one. Each Floquet multiplier is associated with a direction in the Poincaré section as determined by the eigenvectors. The Floquet multipliers may be thought of as gains along each eigenvector direction. The system is stable when the magnitudes of all the eigenvalues are less than unity, which means disturbances are dissipated over subsequent cycles. For more details regarding Floquet multipliers, see [17]. An implicit assumption of calculating Floquet multipliers for walking is that walking is periodic. The relevance of this assumption to walking is detailed in the discussion.

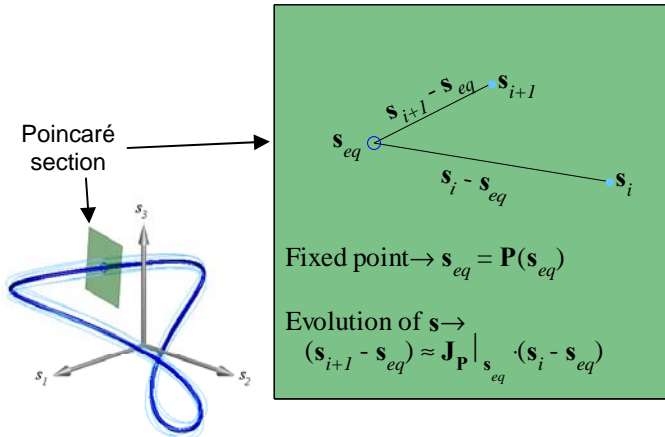


Figure 4. Poincaré section for trajectory  $\mathbf{s}(t)$ .

## 2.3 Experimental data collection and analyses

Nine young adults (two male, seven female,  $23.3 \pm 1.6$  years) completed experimental sessions on three separate days. Their first day included a five minute acclimation to walking in the PAFOs inactive on a treadmill. On day two, subjects walked on the treadmill for a minimum of seven minutes for each PAFO condition: (i) inactive and (ii) active. The order of the conditions was randomized. Their preferred treadmill walking speed was determined for each condition [18]. Before determining their preferred walking speed in the active condition, the control parameters were adapted to align force augmentation with push-off. Following each control parameter adjustment subjects were asked if they would like the treadmill speed changed, since we recognized modification to push-off

power may influence preferred walking speed. Treadmill speed and control parameters were adjusted until the subject no longer requested a speed change and the pneumatic muscles produced forces during push-off. This adjustment process lasted approximately two minutes. Angular velocities of the foot and shank sections of the PAFOs were recorded for one minute of steady-state walking for each condition following the preferred walking speed trials.

Day three included a repeat of day two, followed by measurement of submaximal volumetric rate of oxygen consumption ( $\text{VO}_2$ ) and carbon dioxide production ( $\text{VCO}_2$ ). Submaximal  $\text{VO}_2$  and  $\text{VCO}_2$  were recorded with the treadmill speed at their preferred walking speed for each condition. Additionally,  $\text{VO}_2$  and  $\text{VCO}_2$  were collected while subjects walked in the inactive PAFOs with treadmill speed fixed at their preferred walking speed for the condition. This additional trial eliminated the possible effect of walking at different speeds on metabolic efficiency. In post-comparisons for the inactive condition, metabolic efficiency collected at the inactive and active preferred walking speeds was not different. Therefore, the results presented are for data collected at each subject's preferred walking speed corresponding to PAFO condition.

The one-minute blocks of angular velocity data from days two and three were analyzed independently, since the stability measures require continuous data sets. Angular accelerations of the foot and shank sections were calculated from the angular velocity data. Outcome measures included metabolic efficiency ( $\eta$ ), the maximum Lyapunov exponent ( $\lambda_{\text{max}}$ ), and the maximum Floquet multiplier magnitude ( $\phi_{\text{max}}$ ) for each experimental condition. In post-comparisons, data collected on days two and three did not yield statistically different stability measures and results presented are for the average of these two days.

**Metabolic efficiency.** Metabolic energy expenditure was calculated from the Brockway equation [19] using input values of steady-state  $\text{VO}_2$  and  $\text{VCO}_2$ . Average metabolic energy expenditure during steady-state walking was normalized by body weight and walking speed to yield the dimensionless metabolic cost of transport ( $\text{MCOT}$ :  $\text{W N}^{-1} \text{m}^{-1} \text{s}$ ) [20].  $\text{MCOT}$  represents the amount of energy necessary to carry a unit weight a unit distance.  $\text{MCOT}$  was inverted to yield a dimensionless metabolic efficiency ( $\eta$ :  $\text{N m s}^{-1} \text{W}^{-1}$ ). Greater  $\eta$  values indicate an increase in the distance a unit weight may be moved per unit energy, similar to miles per gallon.

**Dynamic stability.** Both stability indices require a state-space representation of the dynamics of walking. A state vector was constructed from the sagittal plane angular velocities and accelerations of the foot and shank sections of the PAFOs according to,

$$\mathbf{s} = \begin{bmatrix} \dot{\theta}_{lf} & \dot{\theta}_{ls} & \dot{\theta}_{rf} & \dot{\theta}_{rs} & \ddot{\theta}_{lf} & \ddot{\theta}_{ls} & \ddot{\theta}_{rf} & \ddot{\theta}_{rs} \end{bmatrix}^T \quad (4)$$

where the subscripts are abbreviations for  $l$ -left or  $r$ -right, and  $f$ -foot or  $s$ -shank, and the single and double over dots represent first and second derivatives with respect to time. We chose to

use angular velocities and accelerations to avoid non-stationary behavior introduced by integrating velocities over long time periods. Both local and orbital stability are not dependent on the state-basis. Since a smooth coordinate transformation exists between the position-velocity and velocity-acceleration states, the system dynamics are preserved [17].

The maximum Lyapunov exponent,  $\lambda_{\max}$ , was estimated as the mean rate of separation of neighboring trajectories to capture the sensitivity of the dynamic system to perturbations. We modified an algorithm developed by Rosenstein et al. [12] to track the separation of multiple nearest neighbors as opposed to just one. Averaging over multiple nearest neighbors improves the estimate of the maximum Lyapunov exponent. Since we are calculating separation over a finite-time interval, the direction of maximum expansion, corresponding to the maximum Lyapunov exponent, does not have time to “dominate” the dynamics of perturbations in arbitrary directions. Therefore, using only one nearest neighbor for the maximum Lyapunov exponent calculation will underestimate the true maximum unless the nearest neighbor happens to be along the direction of maximum expansion. When multiple nearest neighbors are considered, one is sampling perturbations in multiple state-space directions, increasing the likelihood of a separation in the direction of maximum expansion. For this work we averaged over three nearest neighbors. Ideally, one would like to have nearest neighbors in every state-space direction, but in small experimental data sets, one is limited by the data. We will address the issue of how to best estimate the true finite-time Lyapunov exponent in future work.

Separation was averaged over all points in the data set and  $\lambda_{\max}$  was calculated from a linear fit,

$$\ln(d(t)) = \ln(d_o) + \lambda_{\max} t \quad (5)$$

of the divergence for  $t \in [1, 7]$  seconds.

Calculating Floquet multipliers requires that the state is sampled at a discrete event in the walking cycle [15,16]. We chose to sample the state at left heel-strikes and at right heel-strikes; forming two Poincaré sections. A minimum of 48 consecutive heel-strikes were recorded over the one minute trials for each side. States for each Poincaré section were organized into two matrices for the states at step  $i$ ,  $\mathbf{s}_i$ , and the states at step  $i+1$ ,  $\mathbf{s}_{i+1}$ . A least squares estimate of a linear fit was used to estimate the Jacobian of the Poincaré map,  $\mathbf{J}_p$ ,

$$\mathbf{s}_{i+1} = \mathbf{J}_p \cdot \mathbf{s}_i + \mathbf{\Gamma} \quad (6)$$

where  $\mathbf{\Gamma}$  is a vector of constants [15]. Floquet multipliers,  $\phi$ , were determined by the eigenvalues of  $\mathbf{J}_p$ . To ease comparison between subjects and conditions, we averaged the least stable Floquet multiplier from the left and right heel-strikes. The least stable multiplier is the multiplier with the greatest magnitude,  $\phi_{\max} = \max |\phi|$ .

## 2.4 Statistics

Histograms of the differences in the three outcome measures were examined to determine if the within-subject changes were normally distributed. The differences in the stability measures appeared to violate a normal distribution. Furthermore, because we were interested in testing whether condition (inactive/active) had a positive or negative affect on the outcome measures, we chose to examine differences between conditions with the non-parametric Wilcoxon signed-rank test. For all the tests, statistical significance was defined as  $p \leq 0.05$ . To test the primary hypothesis that providing augmented push-off power increases metabolic efficiency, within subject changes in  $\eta$  were compared to condition (inactive/active). Similarly, for the secondary hypothesis related to stability,  $\lambda_{\max}$  and  $\phi_{\max}$  within subject changes were compared to condition (inactive/active).

## 3 RESULTS

### 3.1 Metabolic efficiency

Eight of the nine subjects increased their metabolic efficiency ( $\eta$ ) when walking with the augmented push-off power provided by the PAFOs (Figure 5, Table 1). Although the data were not normally distributed, we present mean and standard deviation for convenience. On average, efficiency increased by 15 percent when push-off power was augmented. Comparing within-subject changes with the signed rank-test indicated that the increase was a statistically significant effect.

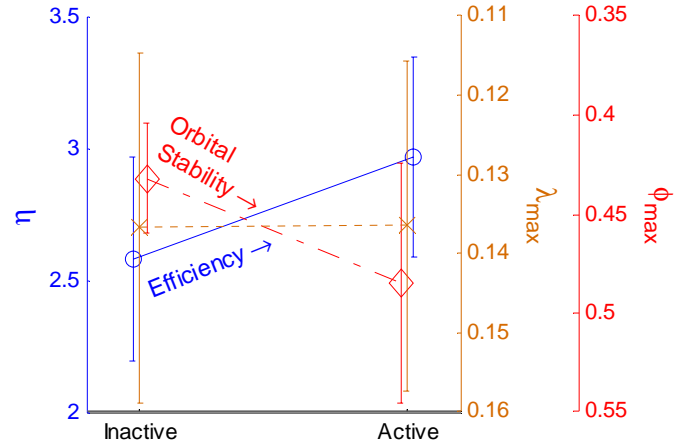


**Figure 5.** Stability (local stability:  $\lambda_{\max}$  dotted; orbital stability:  $\phi_{\max}$  dash-dot) and efficiency ( $\eta$  solid line) results for inactive and active PAFO conditions.

**Table 1.** Efficiency and Stability Results <sup>(a)</sup>

Measure	Condition		With-in Subject Differences	$p^{(b)}$
	Inactive	Active		
$\eta$	$2.58 \pm 0.39$	$2.97 \pm 0.38$	$0.38 \pm 0.30$	<0.01
$\lambda_{\max}$	$0.14 \pm 0.02$	$0.14 \pm 0.02$	$0.00 \pm 0.03$	0.77
$\phi_{\max}$	$0.43 \pm 0.03$	$0.48 \pm 0.06$	$0.05 \pm 0.07$	0.05

<sup>(a)</sup>Data are mean  $\pm$  standard deviation

<sup>(b)</sup> $p$ -values are for within-subject comparisons using Wilcoxon signed rank test

### 3.2 Stability

Examples of each pair of states (angular velocity and respective acceleration) during inactive and active trials are shown in Figure 6. The behavior appears as a noisy limit cycle. Interestingly, the active trials explore a greater region of the state-space. An example of the natural log of the average divergence and the fit of Equation (5) is shown in Figure 7. The maximum Lyapunov exponent increased for five of the nine subjects and decreased for four subjects during walking in the PAFOs active. Thus, no significant trend in local dynamic stability was observed between the two conditions. The maximum of the absolute value of the Floquet multipliers,  $\phi_{\max}$ , increased for seven of the nine subjects during walking with the PAFOs actively augmenting push-off. On average,  $\phi_{\max}$  increased 12 percent. The signed rank-test indicated that the active PAFOs resulted in a statistically significant positive change in  $\phi_{\max}$  (Table 1).

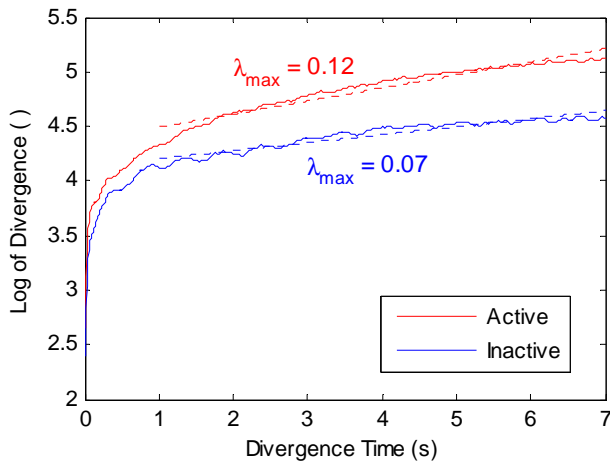


**Figure 7.** Natural log of divergence for a representative inactive and active trial with the linear fit of the maximum Lyapunov exponent for divergence time  $\epsilon \in [1, 7]$  seconds.

### 4 DISCUSSION

We observed that metabolic efficiency increased when the PAFOs were active which supported our primary hypothesis. This result is particularly exciting because it demonstrates that the neuromuscular system was able to adapt to use an external energy source to reduce metabolic cost. The configuration of the pneumatic muscle on the PAFOs simulates the action of the soleus muscle; a muscle that is uni-articular and contributes to plantarflexion. The fact that providing additional energy using a simulated soleus muscle increased metabolic efficiency supports the concept that in healthy adults the ankle plantarflexor muscles contribute to forward locomotion [21-23].

The local stability measures did not indicate a consistent trend between walking with and without the push-off power, while the orbital stability measure indicated decreased stability. The local stability results suggest that, on average, the additional power provided by the PAFOs did not affect how our neuromuscular control responded to small disturbances throughout the walking cycle. Even when the PAFOs were active a majority of the walking cycle, approximately 85 percent, was un-powered. During this un-powered time, we would expect our neuromuscular control response to small disturbances to be the same as when walking in the inactive PAFOs. Since local stability is estimated by averaging throughout the entire cycle, the wearer's neuromuscular control response without power augmentation would likely dominate the average response for the active PAFO condition.

The decrease in orbital stability suggests that the augmented forces decreased the ability of our neuromuscular system to return toward a fixed periodic motion. Recall that the fixed periodic motion is a fixed point on the Poincaré section. This result may also be explained by how we expect our neuromuscular system to respond to augmented forces. Because we did not explicitly control the force profile applied at each push-off, the augmented forces varied between each step. Since our neuromuscular control of walking is plastic [5] the augmented forces most likely resulted in increased variability between steps. If we are not attracting back toward a fixed point, i.e., walking is not a fixed point, but perhaps a *region* on the Poincaré section, then we would expect this greater variability to appear as decreased orbital stability. Nonetheless, this result is still a reason for concern. For the

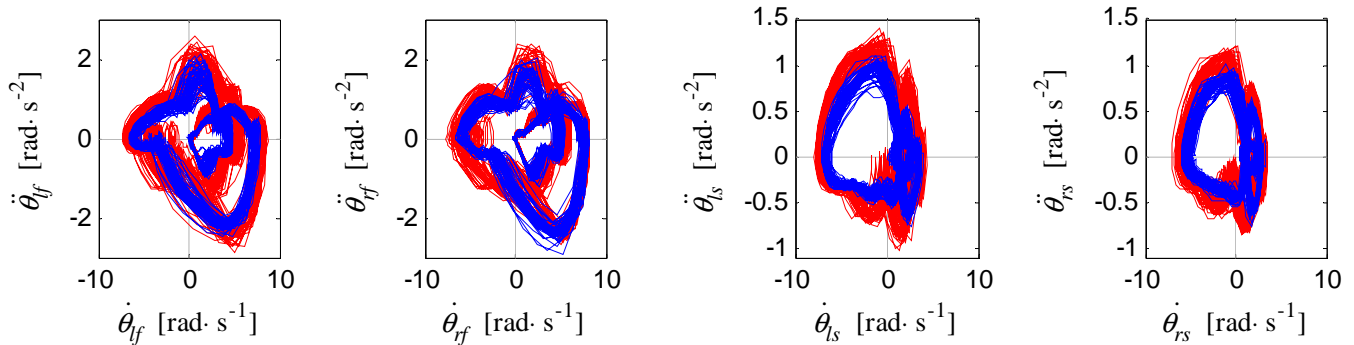


**Figure 6.** Example of the states for a trial where the PAFOs were inactive (blue) and active (red).

algorithm that we used and in other algorithms that rely on the wearer's neuromuscular control for stability, this result could have devastating consequences in movements where the wearer is closer to their limit of stability.

Since none of the subjects we studied actually fell, the decrease in orbital walking stability did not cause a clear functional impairment; subjects were still successfully maintaining stability. In a theoretical system without noise, the increase of 0.05 from the inactive 0.43 maximum Floquet multiplier results in a rapid deviation of disturbance magnitude even over just a few steps. Tracking the same perturbation over two steps the nominal ratio starts at 1:1, shifts to 0.48:0.43, and after the second step, shifts to 0.23:0.18. Interpreting these differences with respect to human locomotion, where the system includes noise in addition to deterministic dynamics, is still an evolving topic.

The population that will ultimately benefit from powered orthoses and prostheses, may have pre-existing musculoskeletal and/or other neurological limitations that may impair the ability to compensate for mechanically induced instabilities. Furthermore, since decreased stability is associated with increased metabolic cost [24], we believe that the best improvement in metabolic efficiency may be reached by a control system that maintains or perhaps even improves movement stability while also providing augmented forces. Thus, stability will become an increasingly important factor to include in the design of powered exoskeletons.

The concept that movement stability is altered by powered exoskeletons has some interesting implications. It has already been demonstrated that our neuromuscular system adapts to augmented forces [5,6]. Thus, it is conceivable that an exoskeleton that improves stability may result in the wearer relying on the stability provided by the exoskeleton. Upon removal of the exoskeleton, the wearer may have lost some of the stability provided by their own neuromuscular system; similar to someone giving up crutches after an extended period of use. This affect could be particularly advantageous in rehabilitation settings. Initially a patient who has suffered an injury and is uneasy with walking or perhaps even unable to walk unassisted, such as following a spinal cord injury or stroke, could wear an exoskeleton to maintain stability. As they progress with re-learning, the effective stability provided by the exoskeleton could be reduced, shifting the regulation of stability from the exoskeleton to the patient's own neuromuscular system.

Our decision to use pneumatic muscles for actuators was based on the fact that they have similar mechanical properties to human muscle [25], making them particularly well suited for the binary ON/OFF control algorithm we used. Their viscoelastic properties smoothed the binary ON/OFF signal to yield a force profile closer to that of the human's natural force production at push-off than the square wave control signal. These actuators were sufficient for demonstrating that metabolic efficiency can be improved when walking in powered exoskeletons. To have a positive affect on stability, we believe it will be necessary to use actuators with larger

bandwidth. At a minimum, we anticipate that we would need to have a response time that is on the order of magnitude of human reflexes [26]. Exoskeletons that use electronic and hydraulic actuators have a much greater bandwidth. In fact, in the BLEEX exoskeleton, which relies on a marginally stable closed loop control system, the time delay and low bandwidth of pneumatic muscles would likely result in instability.

#### **4.1 Limitations**

We acknowledge that the experimental setting was highly controlled and not demanding. In fact, the controller we tested was designed specifically for steady-state walking and was very simple. With the exception of walking straight forward, the controller was not designed to handle any of the typical movements that a person executes over an average day. Much more complex forms of control and actuation exist [1,2]. They allow vastly greater maneuverability and are even self-contained. At this stage, however, our interest was in determining if powered lower extremity exoskeletons have the potential to reduce metabolic cost and how a rudimentary form of positive feedback affected walking stability.

#### **4.2 Future directions**

Ongoing studies are investigating the development of more advanced control algorithms to improve dynamic stability. As pointed out in the discussion, we believe that greater bandwidth than that provided by pneumatic muscles will be necessary to actually improve stability.

### **5 CONCLUSIONS**

Powered orthoses or exoskeleton systems can be used to improve gait performance and efficiency. While walking with a powered ankle-foot orthosis, the metabolic cost of transport was improved by 15% in healthy young adults. However, control mechanisms that include positive feedback for movement or force augmentation may reduce walking stability; in this study statistically significant decreases in orbital stability measures were observed. The functional implications of these changes and the determination of their relationship to actual risk of falling are still ongoing efforts. However, it will become increasingly important to understand how control algorithms for powered devices affect movement stability if we aim to develop powered devices to aid patients with pathologic instability.

### **6 ACKNOWLEDGMENTS**

We would like to acknowledge Melanie Mitros and Erica Byrne for assistance with data collection, Dan Ferris for guidance in developing the PAFOs, Tony Saia and Scott Shaffer at BioTech Prosthetics and Orthotics for helping with construction of the ankle-foot orthoses, and Rod Bradley at Barker Air and Hydraulics for help with the design of the pneumatic system.

We dedicate this paper to the memory of Kevin P. Granata.

## 7 REFERENCES

- [1] Zoss, A. B., Kazerooni, H., and Chu, A., 2006, "Biomechanical design of the Berkeley lower extremity exoskeleton (BLEEX)," *Mechatronics, IEEE/ASME Transactions on*, Vol. 11, No. 2, pp. 128-138.
- [2] Kazerooni, H., 2005, *Exoskeletons for human power augmentation*, pp. 3459-3464. IEEE/RSJ International Conference on Intelligent Robots and Systems (IROS).
- [3] Hayashi, T., Kawamoto, H., and Sankai, Y., 2005, *Control method of robot suit HAL working as operator's muscle using biological and dynamical information*, pp. 3063-3068. IEEE/RSJ International Conference on Intelligent Robots and Systems (IROS).
- [4] Sankai, Y., 2005, *The Leading Edge of Future Technology "Cybernetics": Project HAL - Toward Robot Suits and Cyber Suits?*, pp. xvii. 9th IEEE International Symposium on Wearable Computers.
- [5] Ferris, D. P., Czerniecki, J. M., and Hannaford, B., 2005, "An Ankle-Foot Orthosis Powered by Artificial Pneumatic Muscles," *Journal of Applied Biomechanics*, Vol. 21, No. 2, pp. 189-197.
- [6] Sawicki, G. S., Domingo, A., and Ferris, D. P., 2006, "The effects of powered ankle-foot orthoses on joint kinematics and muscle activation during walking in individuals with incomplete spinal cord injury," *J Neuroengineering.Rehabil.*, Vol. 3, No. 1, pp. 3.
- [7] Guizzo, E. and Goldstein, H., 2005, "The Rise of the Body Bots," *Spectrum, IEEE*, Vol. 42, No. 10, pp. 50-56.
- [8] Dingwell, J. B. and Marin, L. C., 2006, "Kinematic variability and local dynamic stability of upper body motions when walking at different speeds," *Journal of Biomechanics*, Vol. 39, No. 3, pp. 444-452.
- [9] Kang, H. G. and Dingwell, J. B., 2006, "A direct comparison of local dynamic stability during unperturbed standing and walking," *Exp.Brain Res.*, Vol. 172, No. 1, pp. 35-48.
- [10] Buzzi, U. H., Stergiou, N., Kurz, M. J., Hageman, P. A., and Heidel, J., 2003, "Nonlinear dynamics indicates aging affects variability during gait," *Clin.Biomech.(Bristol, Avon.)*, Vol. 18, No. 5, pp. 435-443.
- [11] Wolf, A., Swift, J. B., Swinney, H. L., and Vastano, J. A., 1985, "Determining Lyapunov exponents from a time series," *Physica D: Nonlinear Phenomena*, Vol. 16, No. 3, pp. 285-317.
- [12] Rosenstein, M. T., Collins, J. J., and De Luca, C. J., 1993, "A practical method for calculating largest Lyapunov exponents from small data sets," *Physica D: Nonlinear Phenomena*, Vol. 65, No. 1-2, pp. 117-134.
- [13] Timmer, J., Häussler, S., Lauk, M., and Lücking, C. H., 2000, "Pathological tremors: Deterministic chaos or nonlinear stochastic oscillators?," *Chaos*, Vol. 10, No. 1.
- [14] Franca, L. F. P. and Savi, M. A., 2003, "Evaluating noise sensitivity on the time series determination of Lyapunov exponents applied to the nonlinear pendulum," *Shock and Vibration*, Vol. 10, No. 1, pp. 37-50.
- [15] Hurmuzlu, Y. and Basdogan, C., 1994, "On the measurement of dynamic stability of human locomotion," *J Biomech.Eng*, Vol. 116, No. 1, pp. 30-36.
- [16] Dingwell, J. B., Kang, H. G., and Marin, L. C., 2007, "The effects of sensory loss and walking speed on the orbital dynamic stability of human walking," *J Biomech.*, Vol. 40, No. 8, pp. 1723-1730.
- [17] Nayfeh, A. H. and Balachandran, B., *Applied Nonlinear Dynamics: Analytical, Computational, and Experimental Methods* New York: John Wiley & Sons, Inc., 1995.
- [18] Norris, J. A., Granata, K. P., Mitros, M. R., Byrne, E. M., and Marsh, A. P., 2007, "Effect of augmented plantarflexion power on preferred walking speed and economy in young and older adults," *Gait Posture*, Vol. 25, No. 4, pp. 620-627.
- [19] Brockway, J. M., 1987, "Derivation of formulae used to calculate energy expenditure in man," *Hum.Nutr.Clin.Nutr.*, Vol. 41, No. 6, pp. 463-471.
- [20] Tucker, V. A., 1975, "The energetic cost of moving about," *Am.Sci*, Vol. 63, No. 4, pp. 413-419.
- [21] Neptune, R. R., Kautz, S. A., and Zajac, F. E., 2001, "Contributions of the individual ankle plantar flexors to support, forward progression and swing initiation during walking," *Journal of Biomechanics*, Vol. 34, No. 11, pp. 1387-1398.
- [22] Meinders, M., Gitter, A., and Czerniecki, J. M., 1998, "The role of ankle plantar flexor muscle work during walking," *Scand.J.Rehabil.Med.*, Vol. 30, No. 1, pp. 39-46.
- [23] Eng, J. J. and Winter, D. A., 1995, "Kinetic analysis of the lower limbs during walking: What information can be gained from a three-dimensional model?," *Journal of Biomechanics*, Vol. 28, No. 6, pp. 753-758.
- [24] Donelan, J. M., Shipman, D. W., Kram, R., and Kuo, A. D., 2004, "Mechanical and metabolic requirements for active lateral stabilization in human walking," *Journal of Biomechanics*, Vol. 37, No. 6, pp. 827-835.
- [25] Klute, G. K., Czerniecki, J. M., and Hannaford, B., 2002, "Artificial Muscles: Actuators for Biorobotic Systems," *The International Journal of Robotics Research*, Vol. 21, No. 4, pp. 295-309.
- [26] Matthews, P. B., 1991, "The human stretch reflex and the motor cortex," *Trends Neurosci*, Vol. 14, No. 3, pp. 87-91.